

Thermal and magnetic behaviors of a melt-textured superconducting bulk magnet in the zero-field-cooling magnetizing process

T Oka¹, K Yokoyama², H Fujishiro³ and K Noto³

¹ Faculty of Engineering, Niigata University, 8050 Ikarashi-Nino-cho, Nishi-ku, Niigata 950-2181, Japan

² Ashikaga Department of Electrical and Electronic Engineering, Institute of Technology, 268-1 Ohmae-cho, Ashikaga, Tochigi 326-8558, Japan

³ Faculty of Engineering, Iwate University, 3-4-5 Ueda, Morioka, Iwate 020-8551, Japan

E-mail: okat@eng.niigata-u.ac.jp

Received 15 February 2009, in final form 5 April 2009

Published 19 May 2009

Online at stacks.iop.org/SUST/22/065014

Abstract

The heat generation and magnetic field trapping behaviors of the melt-textured single-domain Sm–Ba–Cu–O bulk superconductor have been precisely investigated in the zero-field-cooling magnetizing processes (ZFC). The temperature and magnetic flux density were simultaneously measured in the temperature range of 50–60 K. Since the invasion of magnetic flux is suppressed by the superconducting pinning effect, the applied magnetic field is not supplied to the whole of the sample. Therefore, the trapped field distributions consequently exhibit trapezoid shapes. According to the balance of heat generation and draining, the temperature profiles show us distinctive behaviors of magnetic fluxes. Both the temperature and the magnetic flux density kept increasing even after the external magnetic field has stopped growing at 5 T. This is attributed to the flux creeping phenomenon which propagates from the periphery to the center portion of the sample like a snow slide. The highest temperature rise due to the flux motion reached 7.5 K even when the sample was magnetized at a slow sweeping rate of 5.06 mT s^{-1} . As the temperature profiles were different between the ascending and descending field processes, it is suggested that the magnetic fluxes invade in and diffuse out in different heating manners between the processes. This assists the hypothesis that the time while the moving fluxes heat the sample strongly affects the total amount of heat generation, which acts contrary to the FC case. This behavior implies that the improvements of the heat propagation property of the HTS bulk material by embedding metallic membranes and more powerful/efficient cooling systems must suppress the temperature increases and enhance the field trapping abilities.

(Some figures in this article are in colour only in the electronic version)

1. Introduction

Melt-textured large grain bulk superconductors composed of $\text{REBa}_2\text{Cu}_3\text{O}_{7-y}$ compounds (RE = Y, Sm, Gd, abbreviated as RE123) which include $\text{RE}_2\text{BaCuO}_5$ (RE211) particles are known to act as quasi-permanent magnets (hereafter referred to as bulk magnets) when they trap the applied magnetic

fields [1, 2]. As reported by Gruss *et al* [3], the maximum trapped field has reached 16 T at 24 K by doping Zn in it. The highest value of 17.24 T has been reported by Tomita *et al* [4], where the Y123 bulk sample was reinforced by the resin impregnation technique. These data of the field trapping ability of bulk magnets are generally measured by the field-cooling method (hereafter abbreviated as FC). Since it is important to

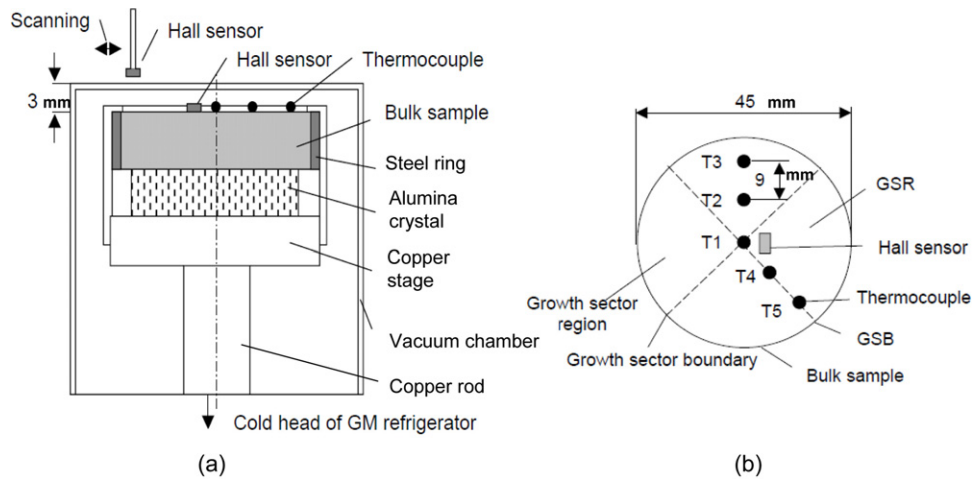


Figure 1. Experimental set-up, (a) a cross-sectional view of the magnetic pole and (b) a top view showing the positions of thermocouples and a Hall sensor on the sample surface.

suppress the heat generation during the activation process, as discussed in this paper, the sweep rates of applied fields must be carefully chosen even in the FC processes using quasi-static fields [5, 6].

In the magnetizing processes using pulsed magnetic fields (PFM), it is known that the flux motion in the sample causes a considerable heating, raises its temperature, lowers the critical current density J_c and subsequently degrades the trapped field ability [7]. Fujishiro *et al* [8, 9] have recently achieved the best performance of a trapped magnetic field of 5.2 T for the first time in the world by a smart process called MMPSC, which is a kind of PFM process. The experiment has been conducted in a manner that suppresses the heat generation by applying iterative pulsed fields at two temperatures. The behavior of invading fluxes is strongly affected by the residual trapped field activated by the former magnetic pulses. They reported that it is important for high field trapping to form an M-shaped magnetic flux distribution before applying intense fields [9].

Zero-field cooling (ZFC) is a kind of magnetizing method to activate the bulk magnets. An intense magnetic field is applied to the sample with low sweep rates in a quasi-static manner after cooling it to the superconducting state. As the flux lines invade the sample through the sample surface, the ZFC technique is regarded as the ultimate model of the PFM methods with extremely slow flux invasion speeds. In a sense, it must be important to know the flux behavior in the ZFC processes so as to obtain excellent trapped field performances in the PFM operations.

In this study, we precisely trace the temperature evolution from the aspect of the phenomena and evaluate the temperature rises due to the heat generation caused by the flux motion in the bulk superconducting magnet during the ZFC processes operated at two initial temperatures of 50 and 60 K.

2. Experimental procedure

2.1. HTS bulk sample and experimental equipment

Illustrations of the experimental set-up are shown in figure 1. A melt-processed high temperature superconducting (HTS)

Sm123 bulk magnet was manufactured by Dowa Mining Co., Ltd and adapted to ZFC operations as well as FC [5, 6]. The dimensions of the sample were 45 mm in diameter and 15 mm in thickness. The sample was reinforced by putting a stainless steel ring on it with epoxy resin to prevent fracture due to the magnetic and thermal stresses during the magnetizing procedures. The trapped field distributions without any strains in FC imply that the material magnetically exhibits a perfect single-domain structure and makes it possible for us to perform the high field trapping ability.

The sample was fixed on the copper stage through an alumina crystal to improve the thermal contact between the copper stage and the bulk sample. The copper stage was connected to the cold head of a compact Gifford–McMahon refrigerator (manufactured by AISIN SEIKI, model GR-103) by a copper heat conduction rod. The nominal output and input powers at 77 K were reported as 15 W and 1000 W, respectively, and the refrigerator enables us to obtain the ultimate temperature of 50 K. The temperature was controlled by a heater which was attached beneath the copper stage. Five pairs of chromel–constantan thermocouples (T1–T5) were separately glued at both positions of a grain sector region (GSR) and a grain sector boundary (GSB) of the polished bulk sample surface, as shown in figure 1(b). The initial temperatures are defined as the averaged data of T1–T5. A Hall sensor (F W Bell, type BHT 921) was attached near the center of the bulk surface to trace the flux behavior during the magnetizing processes and the resultant trapped fields. It must be added that the trapped field data thus obtained do not precisely indicate the maximum trapped fields on the sample surface.

2.2. Procedure

We use a superconducting solenoid magnet with a room temperature bore of 100 mm in diameter, which was manufactured by Japan Superconductor Technology Inc. (type JMTD-5T100). The vacuum chamber containing an HTS bulk sample was inserted into the bore and then the sample was cooled by the GM refrigerator. A static field of 5 T

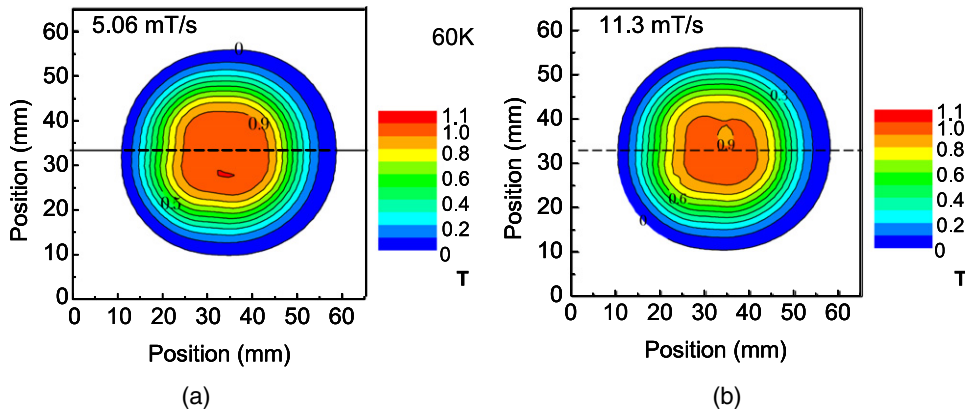


Figure 2. Trapped field distributions of an Sm123 HTS bulk magnet magnetized by a 5 T ZFC process at 60 K at a couple of sweep rates (a) 5.06 and (b) 11.3 mT s⁻¹. Data were measured at 0.5 mm above the magnetic pole surface.

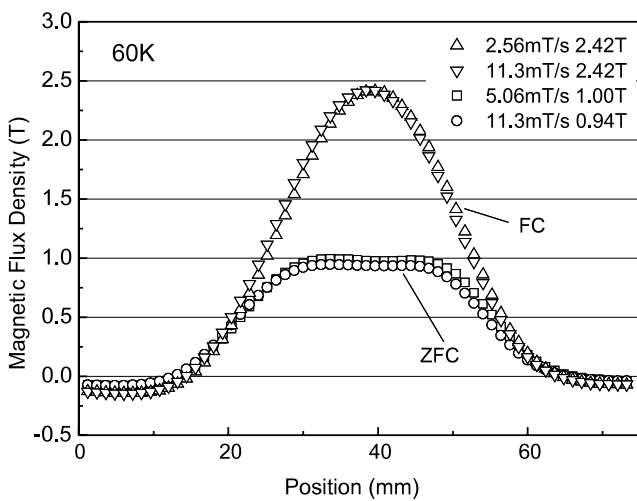


Figure 3. Trapped field distributions after FC and ZFC magnetizing processes at various sweep rates of applied magnetic fields at 60 K.

was gradually applied and subsequently removed with sweep rates of 5.06 and 11.3 mT s⁻¹. The behaviors of temperature and magnetic flux density were precisely measured at the same time throughout the procedure. The magnetic field distributions outside the magnetic pole were measured by scanning a Hall sensor with 0.5 mm gap from the pole surface.

3. Results and discussions

3.1. Distribution of trapped magnetic flux density by ZFC

Figure 2 shows the field distribution maps after ZFC which was operated at 60 K with sweep rates of (a) 5.06 and (b) 11.3 mT s⁻¹ [10]. One can obviously see that the distributions indicate the concentric contour lines. More precisely, these circles slightly deviate towards the outside of the lines which correspond to GSB. This implies that the J_c values at GSB are superior to those in other regions (GSR). The trapped field distributions along the dashed line in figure 2 are shown in figure 3. The profiles obtained by FC are added to them in comparison with ZFC for the same sample. The highest values obtained by ZFC were suppressed to be 1 T, while the

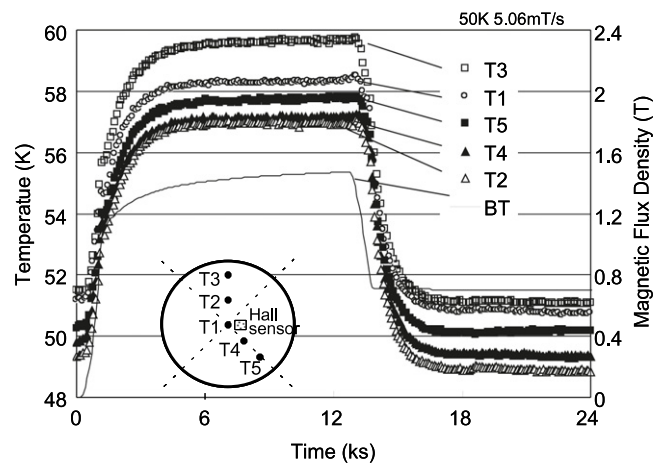


Figure 4. Temperature and trapped field evolution in ZFC at a sweep rate 5.06 mT s⁻¹ at 50 K.

trapped field of 2.42 T was attained in the FC activation by the same applied field of 5 T. As the magnetic field was not satisfactorily given to the whole sample, the magnetic flux could not penetrate into the central portion of it due to the strong pinning effect at around 60 K.

3.2. Time evolution of temperature and trapped magnetic flux

Figure 4 shows the evolution of temperature during the ZFC process in which the sample temperature was controlled to be 50 K. The external field was gradually applied to the sample at a sweep rate of 5.06 mT s⁻¹. The profiles of five thermocouples on the sample surface indicated that all the temperatures simultaneously and uniformly began to rise when the applied magnetic field started rising. This behavior is attributed to the heat generation due to the flux motion in the bulk magnet. As a matter of fact, the temperature data thus measured varied to some extent because of the anticipated calibration errors. All the temperature data soon saturated at the same time when the external field reached 5 T and stopped growing. This saturation implies that the heat generation and draining are almost balanced in the cooling condition given by the GM cryocooler. However, the temperatures have gradually

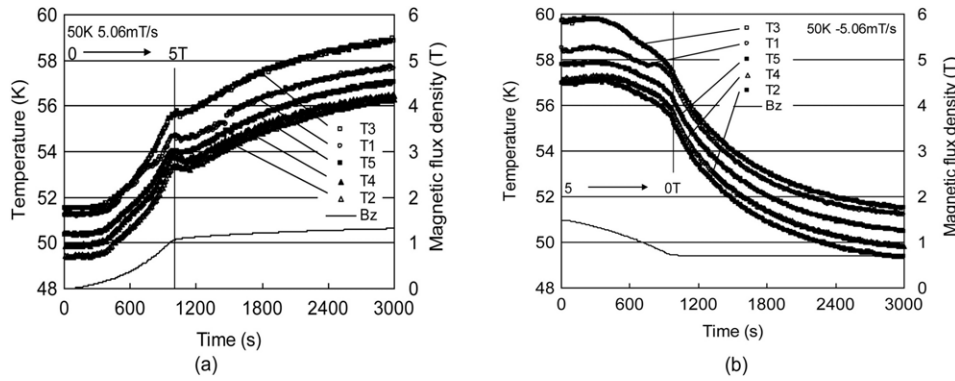


Figure 5. Detailed profiles of figure 4 in (a) ascending and (b) descending field processes at 50 K at a sweep rate of 5.06 mT s^{-1} .

kept rising and the average temperature rise finally reached 7.5 K until the field started decreasing.

We also note that the magnetic flux density B_z has only reached just above 1.4 T in spite of an intense field of 5 T being applied. This is due to the shielding effect of the bulk magnet. The magnetic flux density measured on the sample surface began to rise when the applied magnetic field started rising. Although the profile of the magnetic flux density has also saturated at around 1.2 T when the applied field reached 5 T, it has gradually kept increasing for about two hundred minutes even after the applied field stopped growing as well as the temperature profiles. This implies that the invading fluxes still keep moving towards the central portion of the sample even in the static field. This results in the fact that the distribution of the trapped field exhibits a trapezoid shape after ZFC activation, as shown in figures 2 and 3.

When the external field reached zero, the temperatures sharply fell and returned back to their initial states. This means that heat draining effectively occurs when the heat generation disappears and suggests that the improvement of the heat propagation property of the bulk material would have suppressed the temperature rises more effectively and enhanced the resultant flux trapping ability. Although we have no clear evidence of the position dependence from this rough figure with respect to the measured temperatures, it is inferred that the thermal propagation speed is too fast to recognize the differences among the positions on the sample surface as far as we trace the temperature changes over the timescale of several hundred minutes.

3.2.1. Time evolution of temperature for various sweep rates and temperatures.

Figure 5 shows the detailed thermal changes on its (a) ascending and (b) descending field processes in the ZFC operation which was shown in figure 4. At the very beginning of field application, since the applied weak field is repelled at the sample surface, we can see no distinct temperature rise. After rapid temperature rises which start at 400 s, one sees apparent kinks at 1000 s and the temperatures once again decrease for several hundred seconds. This phenomenon can be understood by an explanation that the heat generation uniformly happens at various portions of the sample, and it diffuses into the various positions of the whole cooling system

including the bulk magnet, the copper cold stage, etc. When the temperature of the whole system becomes stable, it starts rising again, showing the flux creep which propagates from the periphery to the central portion of the bulk magnet. In figure 5(b), the surface temperatures are shown to behave in a fairly balanced way while the external field is decreasing. When the external field reaches zero T, as referred to in the previous paragraph, the temperatures fall steeply at every measuring point. According to the balance between the heating and draining, all the temperature profiles show us a distinctive behavior of the invading fluxes and diffusing heat.

Figure 6 shows the temperature evolution measured at a sweep rate of 11.3 mT s^{-1} . After the drastic temperature rise, the steep peaks appeared at 500 s as well as in the former case in figure 5. This is attributed to the fact that the generated heat propagates through the cooling system at extremely slow speeds for several hundred seconds. This strongly suggests that the heat generation uniformly occurs in every part of the bulk sample surface as long as the applied field is growing at a certain speed and it begins to diffuse into the whole portion of the cooling system when the external field stops rising. As shown in figure 6(b), one can see the steep temperature rise even in the descending field process from 5 to 0 T. This is apparently attributed to the fact that the amount of generated heat is greater than the draining one when the sweep rate is fast.

As the steep temperature rises were observed even on the descending periods in figure 6(b), detailed data for the beginning part is redrawn in figure 7. Among the thermocouples, T5 alone has exhibited a unique temperature gradient. This implies that the heat generation does not equally happen at every point of the sample surface, especially at least in the descending process. It is suggested that the paths of the magnetic fluxes do not uniformly distribute on the sample surface. As far as looking at figure 7, the magnetic fluxes might have avoided position T5 on their way to get out of the sample. T5 corresponds to one of the higher J_c areas on GRB, where the Sm211 inclusions finely reside with higher density than other areas [5, 10].

Figure 8 shows the temperature data which were measured at T1 as functions of the sweep rates and temperature ranges. Although the tendency is apparently the same as that in each temperature range, we can see a big difference between the

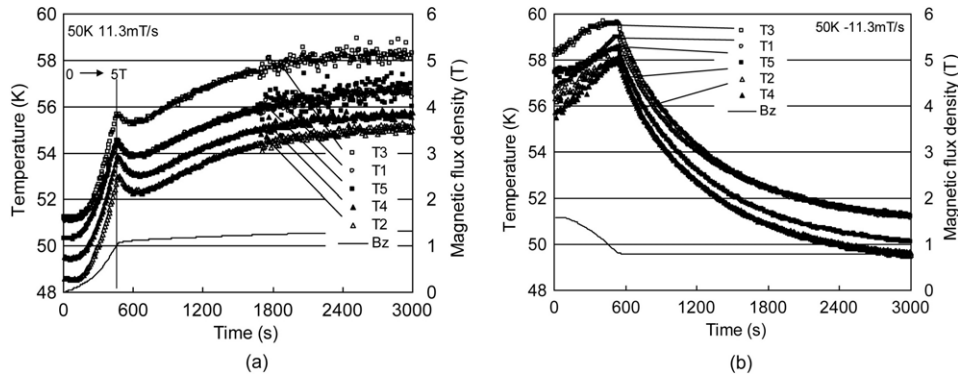


Figure 6. Profiles of (a) ascending and (b) descending field processes at 50 K at a sweep rate of 11.3 mT s^{-1} .

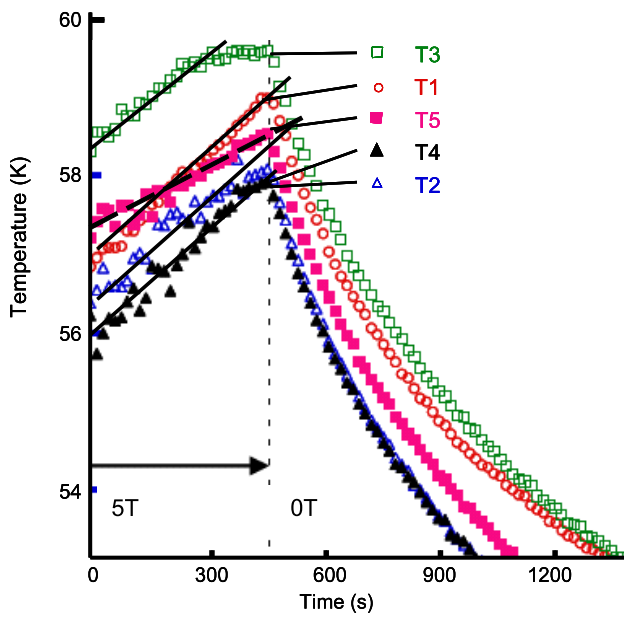


Figure 7. Detailed temperature changes in the descending field process at a rate of -11.3 mT s^{-1} , shown in figure 6(b).

profiles of sweep rates 5.06 and 11.3 mT s^{-1} . It is clear that the temperature rises apparently correspond to the balance of the heat generation rate and the heat draining rate. When the sweep rate is faster, the temperatures would change faster according to the faster heat generation speed while the applied field is sweeping. In the ascending stage, as shown in figure 8(a), the temperature changes are slightly different between the sweeping rates. When the sweep rate is slower, plotted by open symbols, the temperatures reach the slightly higher values at 3000 s than those of the faster rate, shown by closed symbols, in both temperature ranges. This means that the total amount of generated heat during the slower field sweeping is greater than that of the faster one, because the heat draining speeds in each case are the same in both cooling conditions. The duration of heating is responsible for this phenomenon. On the descending stage, figure 8(b), the heat generation rates apparently exceed the draining rates in the faster sweeping process, whereas they show an inverse behavior in the slower sweeping in both temperature ranges. The heat draining speed

corresponds to the heat generation between the sweep rates of 5.06 and 11.3 mT s^{-1} .

3.2.2. Time evolutions of trapped magnetic flux density for various sweep rates and temperatures.

Figure 9 shows the trapped magnetic field data near the center of the sample surface. As shown in figure 9(a), the magnetic flux density has reached over 2 T when the applied field was held at 5 T at 60 K , whereas it was 1.4 T at 50 K . This implies that the shielding effect was weakened at 60 K in comparison with that at 50 K and the flux invasion was allowed to some extent at the higher temperature. At the beginning of the profile, the Hall sensor remained still for a while due to the shielding effect as well as the temperature behavior. As the magnetic fields reached the same data at 3000 s in spite of different sweep rates, the field trapping condition is independent of the sweeping speed and is determined only by the shielding property caused by the pinning effect in the 5 T static field.

In figure 9(b), the resultant trapped fields are observed to be slightly different between the sweep rates. It is understandable that the amount of heat generation apparently affects the remnant trapped fields in the descending field process. As seen in figure 8(b), since the temperatures in the faster processes, noted by closed symbols, during the sweeping time once exceed the profiles of the slower processes at around 500 s , the temperatures which the sample experiences at the faster sweeping rate are higher than those at the slower sweeping rate. This certainly results in different values of the final trapped magnetic flux.

3.3. Estimation of generated heat

As Fujishiro *et al* reported, the heat generation Q is described as follows [11]:

$$Q = \int_{T_s}^{T_s + \Delta T_{\max}} C(T) V dT,$$

where $C(T)$ is the specific heat of the bulk magnet at this temperature range, V is the volume, and T_s and ΔT_{\max} mean the initial temperature and the highest temperature rise, respectively. The specific heat and the heat capacity

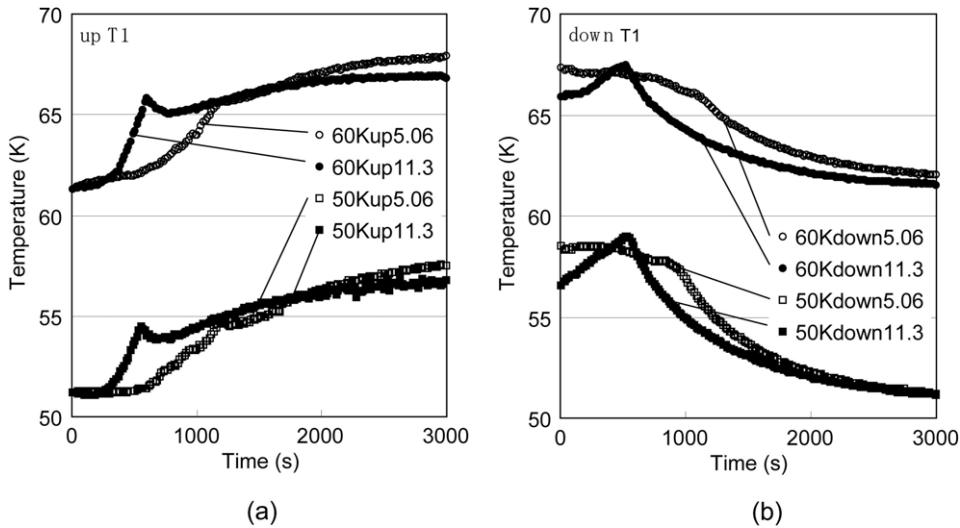


Figure 8. Temperature profiles measured at T1 in (a) ascending and (b) descending field processes as a function of the sweep rate.

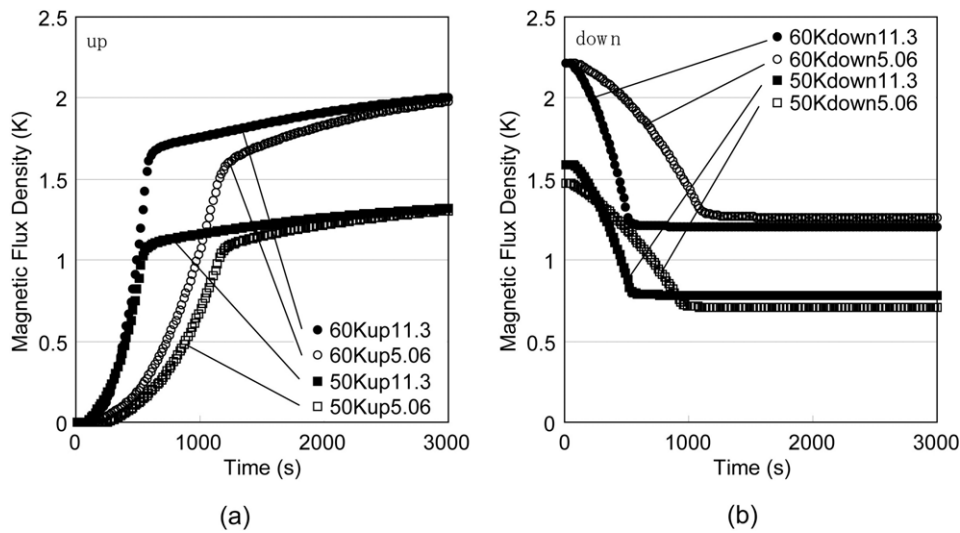


Figure 9. Magnetic field profiles in (a) ascending and (b) descending field processes.

of bulk magnets at around 50 K are estimated as $0.8 \times 10^{-3} \text{ J mm}^{-3} \text{ K}^{-1}$ [11] and 19 J K^{-1} , respectively, whereas the volume of the sample is $23.8 \times 10^3 \text{ mm}^3$. As the cooling rate is derived to be 0.01 K s^{-1} from figure 7, the calculated heat draining of 0.19 W mainly corresponds to 2.7% of the cooling power of the GM cryocooler, which nominally generates 7 W at 50 K [12]. The major portion of cooling energy is spent on heat draining against the heat invasion from outside the vacuum insulation system.

3.4. Temperature changes

Figure 10 shows the temperature rise as functions of various sweep rates, positions and initial temperatures. The FC data, denoted as (+), were added for comparison with the ZFC in the figure. The highest value of the averaged temperature rises was recorded as 7.5 K, which was obtained when the process was operated at the slow sweep rate of 5.06 mT s^{-1} at 50 K.

This assists the hypothesis that the time period being heated by the moving fluxes strongly affects the total amount of heat generation, which acts contrary to the FC case. As the different behaviors of the temperature changes were observed between its ascending and descending field processes, it is suggested that the magnetic fluxes invade in and diffuse out in different manners between their ascending and descending stages. It is also inferred that the difference between the specific heats at 50 and 60 K must correspond to the temperature rises at the slow sweeping rate.

Figure 11 shows the averaged temperature changes during the ascending and descending periods as functions of the initial cold head temperatures and the sweep rates. The data shows a good example to imply that there are different behaviors between slow and fast sweep rates in the descending stage. In the field ascending period, closed notes, heat generation is mainly caused on the periphery of the sample and propagates to the central portion. Then we do not see any substantial

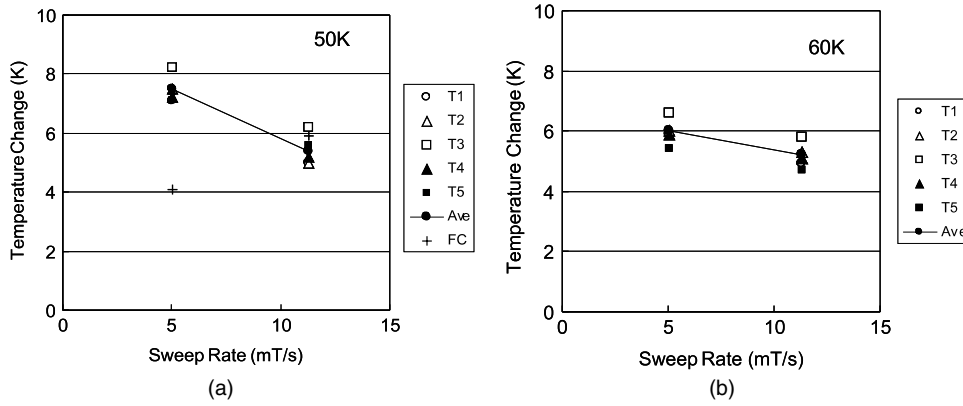


Figure 10. Maximum temperature rises at various positions of thermocouples against sweep rates in ZFC cooled to (a) 50 K and (b) 60 K.

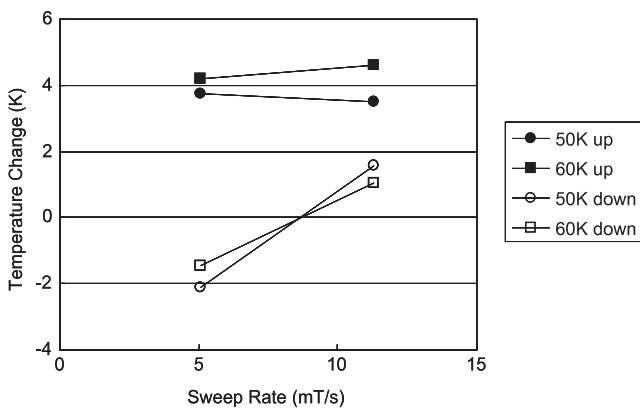


Figure 11. Averaged temperature changes during ascending field (up) and descending field (down) periods in ZFC at 50 and 60 K.

Table 1. Temperature changes (K) measured on the bulk sample surface. (Note: T_i : initial temperature, R_s : sweep rate, T_{ave} : averaged data, T_{FC} : compared with field-cooling method [5].)

T_i	R_s (mT s ⁻¹)	T1	T2	T3	T4	T5	T_{ave}	T_{FC}
50	5.06	7.1	7.5	8.2	7.2	7.4	7.5	4.1
50	11.3	5.0	5.0	6.2	5.2	5.6	5.4	5.9
60	5.06	5.9	6.0	6.6	5.9	5.4	6.0	—
60	11.3	4.9	5.3	5.8	5.1	4.7	5.2	—

differences between the temperatures nor sweep rates. In the descending time, however, when the sweep rate is slow, the heat generation is much weaker than that of the faster one. The sweep rate affects the temperature rise because the temperature change depends on the balance between heat generation and draining. Noudem *et al* [13] reported that embedding metal membranes into the holes which were drilled in the samples is effective at improving the mechanical strength of the materials. Thanks to the heat conduction property of metals, the heat draining of such samples would be improved, and it would be possible to reduce their heating up during the magnetizing processes. The data of temperature changes are listed in tables 1 and 2, which correspond to figures 10 and 11.

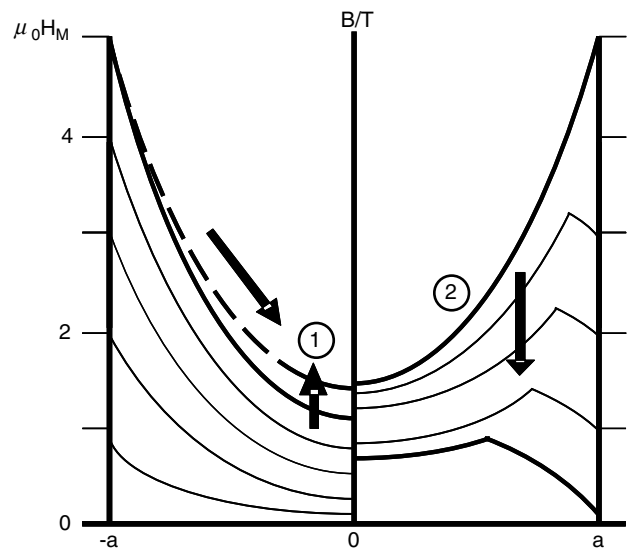


Figure 12. Illustration of the magnetic flux behavior.

Table 2. Temperature changes (K) during sweeping magnetic field. (Note: R_s : sweep rate, up: ascending field, down: descending field.)

R_s (mT s ⁻¹)	50 K up	60 K up	50 K down	60 K down
5.06	3.8	4.2	-2.1	-1.4
11.3	3.5	4.6	1.6	1.0

3.5. Behavior of trapped magnetic flux

The schematic illustration which explains the flux motion in the sample is shown in figure 12. The ascending and descending magnetic flux are indicated on the left- and right-hand sides of the figure, respectively. When the field is initially applied, the fluxes are prevented from invading the sample. When the field reaches 5 T, the magnetic fluxes still keep penetrating into the sample even after the external field stops increasing, and fall into the central portion, showing a flux creeping phenomenon like a snow slide. This flux creeping releases the fluxoids from the pinning centers and then generates the heat which corresponds to the pinning energy. So we can trace the specified paths through which the magnetic fluxes disperse out of the sample by measuring the temperature distribution.

On the descending stage from 5 T to zero, since the central portion of the sample is shielded by the surrounding fields and the heat generation is not intense in the high field region over 2 T, the trapped field in the center tends to keep its value and sluggishly decreases as if it were frozen. Therefore, this behavior of the magnetic flux results in the trapezoid or M-shaped distribution after the ZFC operation, whereas they show a cone shape when magnetized in the FC process.

The inhomogeneous temperature and flux distributions in the bulk sample have been reported by Laurent *et al* [14] with respect to the weak ac field application. They have pointed out that the trapped dc field before ac field application reduces the temperature increases. This is another example of heat generation by the flux motion in bulk samples.

4. Conclusions

The temperature rises of an Sm–Ba–Cu–O single-domain bulk superconductor have been precisely measured during the ZFC process. The highest temperature rise has been reported as 7.5 K when the sample was magnetized at a sweeping rate of 5.06 mT s^{-1} at 50 K. We have so far emphasized that the temperature change is never negligible even in the ZFC magnetizing operation as well as the FC. The conclusions of this study are listed as follows.

Both the temperatures and the magnetic fields have gradually kept increasing even after the applied magnetic field stopped growing at 5 T. The magnetic fluxes fall into the central portion of the sample even in the static field, showing the flux creeping like a snow slide.

It is clarified that the time period while being heated by the moving fluxes strongly affects the total amount of heat generation, which acts contrary to the FC case. Different temperature gradients were observed in its descending period, which inferred the presence of various heat draining paths through which the magnetic fluxes diffuse outside. It is also suggested that the paths of invading and diffusing fluxes are different between its ascending and descending processes.

The trapped field distribution which exhibits a trapezoid shape was discussed and consistently explained by flux motions during the ZFC process. This behavior implies that the improvements of the heat propagation property of the HTS bulk materials and the cooling systems must suppress the temperature increases and enhance the resultant flux trapping abilities.

Acknowledgments

This work has been partially supported by grants-in-aid from the Japan Science and Technology Agency (JST) and Iwate Industrial Promotion Centre.

References

- [1] Wipf S and Laquer H 1989 Superconducting permanent magnet *IEEE Trans. Magn.* **25** 1877–80
- [2] Weinstein R, Chen I-G, Liu J and Lau K 1991 Permanent magnets composed of high temperature superconductors *J. Appl. Phys.* **70** 6501–3
- [3] Gruss S, Fuchs G, Krabbes G, Verges P, Stover G, Muller K, Fink J and Schultz L 2001 Superconducting bulk magnets: very high trapped fields and cracking *Appl. Phys. Lett.* **79** 3131–3
- [4] Tomita M and Murakami M 2003 High-temperature superconductor bulk magnets that can trap magnetic fields of over 17 tesla at 29 K *Nature* **421** 517–20
- [5] Oka T, Yokoyama K, Fujishiro H, Kaneyama M and Noto K 2005 Temperature changes in a melt-processed YBCO superconductor activated by field cooling magnetization process *Physica C* **426–431** 794–9
- [6] Oka T, Yokoyama K, Fujishiro H and Noto K 2007 Temperature rise in melt-textured large grain superconducting bulk magnets during their magnetizing operations *Physica C* **460–462** 748–9
- [7] Itoh Y and Mizutani U 1996 Pulsed field magnetization of melt-processed Y–Ba–Cu–O superconducting bulk magnet *Jap. J. Appl. Phys.* **35** 2114–25
- [8] Fujishiro H, Kaneyama M, Tateiwa T and Oka T 2005 Record-high trapped magnetic field by pulse field magnetization using GdBaCuO bulk superconductor *Japan. J. Appl. Phys.* **44** L1221–4
- [9] Fujishiro H, Tateiwa T, Fujiwara A, Oka T and Hayashi H 2006 Higher trapped field over 5 Tesla on HTSC bulk by modified pulse field magnetization *Physica C* **445–448** 334–8
- [10] Oka T, Yokoyama K, Fujishiro H and Noto K 2009 Thermal behavior and field-trapping property of melt-textured superconducting bulk magnets activated by quasi-static magnetic fields *LT25: 25th Int. Conf. on Low Temperature Physics (Aug. 2008)* p LT1366; *J. Phys.: Conf. Ser.* **150** 052195
- [11] Fujishiro H, Kaneyama M, Yokoyama K, Oka T and Noto K 2005 Generated heat during pulse field magnetizing for REBaCuO (RE = Gd, Sm, Y) bulk superconductors with different pinning abilities *Supercond. Sci. Technol.* **18** 158–65
- [12] Oka T, Hirose Y, Kanayama H, Kikuchi H, Fukui S, Ogawa J, Sato T and Yamaguchi M 2007 Performances of compact magnetic field generators using cryo-cooled high temperature bulk superconductors as quasi-permanent magnets *Supercond. Sci. Technol.* **20** 1233–8
- [13] Noudem J, Meslin S, Horvath D, Harnois C, Chateigner D, Eve S, Gomina M, Chaud X and Murakami M 2007 Fabrication of textured YBCO bulks with artificial holes *Physica C* **463–465** 301–8
- [14] Laurent Ph, Vanderbenden Ph, Meslin S, Noudem J, Mathieu J, Cloots R and Ausloos M 2007 Measurements of thermal effects in a bulk YBCO single domain superconductor submitted to a variable magnetic field *IEEE Trans. Appl. Supercond.* **17** 3036–9